J. Cent. South Univ. (2020) 27: 1770−1779
DOI: https://doi.org/10.1007/s11771-020-4406-y

Springer

A comprehensive comparative investigation of frictional force models for dynamics of rotor−bearing systems

LIU Jing(刘静)[1,2]

1. School of Marine Science and Technology, Northwestern Polytechnical University, Xi'an 710072, China;
2. Laboratory for Unmanned Underwater Vehicle, Northwestern Polytechnical University, Xi'an 710072, China

Abstract: Vibrations of a rotor-bearing system (RBS) can be affected by the frictional forces between the components of the inherent bearings. Thus, an in-depth investigation of the influences of the frictional moments of the bearings on the vibrations of the RBS can be helpful for understanding the vibration mechanisms in the rotating machinery. In this study, an improved dynamic model of a RBS considering different frictional force models is presented. A comparative investigation on the influences of the empirical and analytical frictional force models on the vibration characteristics of the RBS is proposed. The empirical frictional force models include Palmgren's and SKF's models. The analytical frictional force model considers the rolling friction caused by the radial elastic material hysteresis, slipping friction between the ball and races, viscosity friction caused by the lubricating oil, and contact friction between the ball and cage. The influences of the external load and rotational speed on the vibrations of the RBS are analyzed. The comparative results show that the analytical frictional force model can give a more reasonable method for formulating the effects of the friction forces in the bearings on the vibrations of the RBS. The results also demonstrate that the friction forces in the bearings can significantly affect the vibrations of the RBSs.

Key words: friction force; vibrations; rotor-bearing system; dynamic model

Cite this article as: LIU Jing. A comprehensive comparative investigation of frictional force models for dynamics of rotor−bearing systems [J]. Journal of Central South University, 2020, 27(6): 1770−1779. DOI: https://doi.org/10.1007/s11771-020-4406-y.

1 Introduction

Rotor-bearing systems (RBSs) are essential components in various rotating machinery. The operational accuracy and vibration performances of the RBSs are greatly affected by the dynamic contact and frictional forces in their inherent bearings [1, 2]. Therefore, an investigation of the frictional force models for dynamics of the RBSs can be useful for analyzing the vibrations of the rotating machinery.

Many works studied the frictional forces in rolling element bearings (REBs). PALMGREN [3] introduced an empirical method to study the frictional forces in REBs. DENG et al [4], KAKUTA [5] and SNARE [6−8] analyzed the effects of the elastic material hysteresis, hydrodynamic lubrication, slipping and spinning on the frictional forces in ball bearings. TODD et al [9] used an experimental method to study the groove radius on the frictional forces of angular ball bearings. GENTLE et al [10] considered the frictional forces between the cage and other bearing components in their frictional force model. TRIPPETT [11] studied the effects of the lubrication and radial load on the frictional forces of the needle and ball bearings by using an

Foundation item: Projects(51605051, 51975068) supported by the National Natural Science Foundation of China; Project(3102020HHZY030001) supported by the Fundamental Research Funds for the Central Universities, China
Received date: 2020-01-18; **Accepted date:** 2020-03-11
Corresponding author: LIU Jing, PhD, Professor; Tel: +86-13658335960; E-mail: jliu0922@nwpu.edu.cn, jliu@cqu.edu.cn; ORCID: 0000-0003-2323-3475

experimental method. CHIU et al [12] conducted an empirical method for calculating the frictional forces of the needle bearings. Svenska Kullager Fabriken (SKF) Group [13] introduced an empirical method based on the experimental results for calculating the frictional forces model for the REBs. IQBAL et al [14] studied the lubrications on the frictional forces of the needle bearings by using an experimental method. They found that the results from the experiment and empirical methods (Palmgren's and SKF's methods) have a great difference. LIU et al [15, 16] presented a new model to formulate effect of the roundness error on the friction torques in a roller bearing and ball bearing. TONG et al [17] introduced a simulation method to study the friction moments of an angular contact ball bearing with the angular misalignment. HAN et al [18, 19] studied the frictional and vibration characteristics of the ball bearings. XU et al [20] presented a friction forces analysis of a double-row tapered roller bearing. KWAK et al [21] conducted a cryogenic friction method to study the dynamic performance of a ball bearing. The above listed works introduced many empirical and analytical methods to formulate the frictional forces in different rolling element bearings. However, the vibrations of the bearings caused by the frictional forces were not studied.

Moreover, some works have been reported to analyze the effect of the frictional forces on the vibrations of the rolling element bearings. BABU et al [22, 23] developed a dynamic model combined with Palmgren's frictional force model to discuss the effect of the frictional forces on the vibrations of a rotor-bearing system. LIU et al [24, 25] developed the finite element model combined with the Coulomb frictional model to study the effect of the local defects on the vibrations of the bearings. CAO et al [26, 27] proposed different dynamic models to study the local faults on the dynamic forces and vibrations of bearings. HALMINEN et al [28] presented a new model to formulate the dynamic frictional forces in a touchdown bearing with the surface waviness. LIU et al [29, 30] conducted a new dynamic model combined with Palmgren's frictional force model to study the effect of the local defects on the vibrations of a rotor-bearing system. NEISI et al [31] established a dynamic and thermal model to formulate the frictional forces and heat generation in a touchdown bearing with the surface waviness. XU et al [32] discussed the dynamic contact and frictional forces in a bearing-cycloid-pinwheel transmission system. ZHENG et al [33] developed an experimental and numerical methods to study the vibrations on the friction moment of an angular contact ball bearing. POPESCU et al [34] discussed four approaches for predicting the friction moment in a ball bearing. HAMMAMI et al [35] studied the friction moment of a rolling bearing with the axle gear oil. ZHANG et al [36] studied the waviness error on the friction moment of a ball bearing. MAJDOUB et al [37] used experimental and numerical methods to study the friction moment in a tapered roller bearing. The above listed works only used the empirical Palmgren's and simple Coulomb models to formulate the frictional forces in their dynamic models. As the analysis in Ref. [15], the differences of the frictional forces from the classic Palmgren's, SKF's, and analytical methods are very large. The different frictional forces should produce different system vibrations. Thus, the goal of this work is to give a comprehensive comparative investigation of the frictional force models for dynamics of the RBSs.

This study provides an improved dynamic model combined different frictional force models to study the effect of the frictional force in the inherent ball bearings on the vibrations of an RBS. The improved dynamic model in this study is partially based on the modelling method in Ref. [29]. However, Ref. [29] only used the Palmgren's empirical model in their dynamic model, which cannot accurately describe the friction forces in the bearing according to the analysis results in Ref. [15]. Thus, the dynamic model in Ref. [29] is improved to consider the empirical and analytical friction force models, which was not reported in the listed literature. Palmgren's, SKF's, and analytical frictional force models in the previous works are studied in this work. The results from Palmgren's, SKF's, and analytical friction force models have been compared to validate a more reasonable friction force model for calculating the friction forces in rolling element bearings as given in Ref. [15]. Moreover, in Refs. [15] and [16], the simulation results from the above three methods were compared with those from IQBAL et al [14]. The compared results show that the analytical method is

a more reasonable one for calculating the friction forces of the rolling element bearings due to the centrifugal forces and dynamic contact forces between the mating parts of the bearing, especially for a higher rotating speed. However, Refs. [15] and [16] did not study the effect of the friction force on the vibrations of the rotor system. Furthermore, the support stiffnesses of the housing are considered in the model. The lubrication conditions in the bearings are also formulated. A Runge−Kutta method is applied to obtain the results from the dynamic model. The vibrations of the RBS from the dynamic models with different frictional forces models in the previous literature are compared.

2 Model description

2.1 Frictional force models

The analytical models in the previous works and empirical models including Palmgren's and SKF's models are used. The details of the models are briefly listed as follows. Since the bearing system in this work is defined as the oil lubricating condition, the values of the coefficients in the Palmgren's model and SKF model are used.

2.1.1 Palmgren's model

The load dependent and independent factors are considered in Palmgren's model. The equation of Palmgren's model is expressed as [3]:

$$M_{\mathrm{Palm}} = M_0 + M_1 \tag{1}$$

where M_0 is the load independent factor. It is given by:

$$M_0 = \begin{cases} 10^{-7} f_0 (\nu n)^{\frac{2}{3}} D^3, & \nu n \geq 2000 \\ 160\times 10^{-7} f_0 D^3, & \nu n < 2000 \end{cases} \tag{2}$$

where f_0 is the lubricant coefficient, the value of which is chosen to be 1.5 in this work [38]. n is the rotor velocity; ν is the kinematic viscosity; and D is the bearing pitch diameter. Furthermore, M_1 is the load dependent factor, which is given as:

$$M_1 = f_1 \cdot P \cdot D \tag{3}$$

where f_1 is a factor based on the bearing force and design geometries; and P is the applied force, which is equal to $0.9F_{\mathrm{a}}\cos\alpha - 0.1F_{\mathrm{r}}$, where F_{a} and F_{r} are the axial and radial forces.

2.1.2 SKF's model

The rolling, slipping, seal, and viscous frictional forces are empirically considered in SKF's model. The equation of SKF's model is given by [13]:

$$M_{\mathrm{SKF}} = \varphi_1\varphi_2 M_{\mathrm{rS}} + M_{\mathrm{sS}} + M_{\mathrm{eS}} + M_{\mathrm{vS}} \tag{4}$$

where φ_1 and φ_2 are the small oil backfill reduction and shear heat reduction factors, respectively. The rolling friction torque M_{rS} is written as:

$$M_{\mathrm{rS}} = G_{\mathrm{rS}} (\nu n)^{0.6} \tag{5}$$

where G_{rS} is a factor based on the bearing geometries and forces. The slipping friction torque M_{sS} is given as:

$$M_{\mathrm{sS}} = \mu_{\mathrm{sS}} G_{\mathrm{sS}} \tag{6}$$

where μ_{sS} is the slipping friction parameter, which is 0.02 in this study; and G_{sS} is a slipping friction factor based on the bearing types. The seal friction torque M_{ef} is given by:

$$M_{\mathrm{ef}} = K_{\mathrm{s1}} \cdot d_{\mathrm{s}}^{\beta} + K_{\mathrm{s2}} \tag{7}$$

where K_{s1}, K_{s2} and β are the fixed coefficients; and d_{s} is the contact area diameter between the seal and bearing ring. The viscous friction torque M_{vS} is given as:

$$M_{\mathrm{vS}} = 10 V_{\mathrm{m}} K_{\mathrm{roll}} B D^4 n^2 \tag{8}$$

where V_{m} is the drag loss parameter, which is 0.00005 in this study; B is the inner ring width; and K_{roll} is a fixed drag loss parameter.

2.1.3 Analytical model

The rolling, slipping, seal, and viscous are also analytically considered in the analytical model. The equation of the analytical model is given as [15]

$$M_{\mathrm{Am}} = M_{\mathrm{eA}} + M_{\mathrm{sA}} + M_{\mathrm{cA}} + M_{\mathrm{dA}} \tag{9}$$

where M_{eA} is the rolling friction torque. It is given by:

$$M_{\mathrm{eA}} = \sum_{j=1}^{Z} \left(\frac{2a_{\mathrm{h}} Q_{ij} b_{ij}}{3\pi R} + \frac{2a_{\mathrm{h}} Q_{oj} b_{oj}}{3\pi R} \right) \frac{D}{2} \tag{10}$$

where Z is the number of the ball; a_{h} is the elastic hysteresis coefficient, which is 0.01; R is the ball radius; b_{ij} and b_{oj} are the contact area radii for the inner and outer rings, respectively; Q_{ij} and Q_{oj} are the contact loads for inner and outer rings, respectively. The differential slipping friction torque M_{sA} is given as:

$$M_{\mathrm{sA}} = \sum_{j=1}^{Z} \left(2\int_0^{b_{ij}} \mu_{\mathrm{si}} Q_{ij} \mathrm{d}b \cdot \frac{D - D_{\mathrm{b}}}{2} + \right.$$

$$2\int_0^{b_{oj}} \mu_{so} Q_{oj} \mathrm{d}b \frac{D+D_b}{2}\Bigg) \tag{11}$$

where μ_{si} and μ_{so} are the slipping friction factors for the inner and outer rings, respectively; and D_b is the ball diameter. The friction torque between the ball and cage M_{cA} is given by:

$$M_{cA} = \frac{\omega_b D_b \sum_{j=1}^{Z} \mu_c F_{cj}}{2\omega_r} \tag{12}$$

where ω_b is the ball spin velocity; μ_c is the friction factor between one ball and cage; ω_r is the rotor velocity; and F_{cj} is the contact force between one ball and cage. The viscosity friction torque M_{dA} is given as:

$$M_{dA} = \sum_{j=1}^{Z} \frac{1}{8} C_d \rho_0 D_w l (D\omega_c)^2 \frac{D}{2} \tag{13}$$

where C_d is the drag factor, which is 3.0; ω_c is the cage velocity; and ρ_0 is the oil density.

2.2 Dynamic model

A lumped spring-mass model for the studied RBS is given in Figure 1. The rotor weight is defined as $M_{ri}g$. The axial preload is applied along z direction. The transverse, longitudinal, and rotational displacements along x, y and z directions are considered. The model is applied to analyzing the effects of the frictional forces in the bearings on vibrations of the RBS.

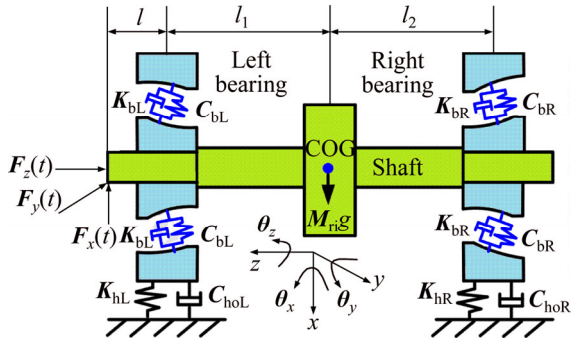

Figure 1 A rigid rotor–ball bearing system

The dynamic model of the RBS presented by Ref. [29] is improved to consider different frictional force models. The equation of the translational motions of the rotor is expressed as:

$$[\boldsymbol{M}_r]\{\ddot{\boldsymbol{q}}_r\} + [\boldsymbol{C}_{bL}]\{\dot{\boldsymbol{q}}_r - \dot{\boldsymbol{q}}_{hL}\} + [\boldsymbol{C}_{bR}]\{\dot{\boldsymbol{q}}_r - \dot{\boldsymbol{q}}_{hR}\} = -\Delta_L\{\boldsymbol{F}_{bL}\} - \Delta_R\{\boldsymbol{F}_{bR}\} + \zeta\{\boldsymbol{G}\} - \{\boldsymbol{F}_a\} \tag{14}$$

where $\boldsymbol{M}_r$ and $\boldsymbol{q}_r$ are the rotor mass matrix and displacement vector, respectively; $\boldsymbol{C}_{bL}$ and $\boldsymbol{C}_{bR}$ are the damping matrices of the left and right bearings, respectively; $\boldsymbol{q}_{hL}$ and $\boldsymbol{q}_{hR}$ are the displacement matrices of the left and right bearing housings, respectively; Δ_L is the force parameter for left bearing, whose value is $\cos\alpha_i\cos\theta_i$, $\cos\alpha_i\sin\theta_i$ and $\sin\alpha_i$ for x, y and z directions, respectively; α_i and θ_i are the contact angle and angular position of ith ball of the left bearing, respectively; Δ_R is the force parameter for the right bearing, whose value is $\cos\alpha_j\cos\theta_j$, $\cos\alpha_j\sin\theta_j$ and $\sin\alpha_j$ for x, y and z directions, respectively; α_j and θ_j are the contact angle and angular position of jth ball of the right bearing, respectively; $\boldsymbol{F}_{bL}$ and $\boldsymbol{F}_{bR}$ are the total contact force matrices in the left and right bearings matrices, respectively; $\boldsymbol{G}$ is the rotor weight vector; ζ is gravity parameter, whose value is 1, 0 and 0 for x, y and z directions, respectively; and $\boldsymbol{F}_a$ is the applied load vector. The equation of the left housing is given as:

$$[\boldsymbol{M}_{hL}]\{\ddot{\boldsymbol{q}}_{hL}\} + [K_{hL}]\{\boldsymbol{q}_{hL}\} + [\boldsymbol{C}_{hL}]\{\dot{\boldsymbol{q}}_{hL}\} - [\boldsymbol{C}_{bL}]\{\dot{\boldsymbol{q}}_r - \dot{\boldsymbol{q}}_{hL}\} = \Delta_L\{\boldsymbol{F}_{bL}\} \tag{15}$$

where $\boldsymbol{M}_{hL}$ and $\boldsymbol{q}_{hL}$ are the left housing mass matrices; $\boldsymbol{C}_{hL}$ is the damping matrix of the left housing; and $\boldsymbol{K}_{hL}$ is the stiffness matrix of the left housing. The equation of the right housing is written as:

$$[\boldsymbol{M}_{hR}]\{\ddot{\boldsymbol{q}}_{hR}\} + [K_{hR}]\{\boldsymbol{q}_{hR}\} + [\boldsymbol{C}_{hR}]\{\dot{\boldsymbol{q}}_{hR}\} - [\boldsymbol{C}_{bR}]\{\dot{\boldsymbol{q}}_r - \dot{\boldsymbol{q}}_{hR}\} = \Delta_R\{\boldsymbol{F}_{bR}\} \tag{16}$$

where $\boldsymbol{M}_{hR}$ and $\boldsymbol{q}_{hR}$ is the right housing mass matrices; $\boldsymbol{C}_{hR}$ is the damping matrix of the left housing; and $\boldsymbol{K}_{hR}$ is the stiffness matrix of the left housing. Moreover, the equation of the rotational motions of the rotor is given by:

$$[\boldsymbol{I}_r]\{\ddot{\boldsymbol{\theta}}_r\} - [\boldsymbol{I}_{re}]\{\ddot{\boldsymbol{\theta}}_{r1}\}\{\ddot{\boldsymbol{\theta}}_{r2}\} = \eta_1 l_1 \Delta_{L1}\{\boldsymbol{F}_{bL}\} + \{\boldsymbol{M}_f\} + \eta_2 l_2 \Delta_{R1}\{\boldsymbol{F}_{bR}\} + \frac{D\Delta_{L2}}{2}\{\boldsymbol{F}_{bL}\} - \frac{D\Delta_{R2}}{2}\{\boldsymbol{F}_{bR}\} \tag{17}$$

where $\boldsymbol{I}_r$ is the inertia moment of the rotor about different axes; $\boldsymbol{I}_{re}$ is the I_y-I_z, I_z-I_x, and I_x-I_y for x, y and z directions, respectively; η_1 is 1, −1 and 0 for x, y and z directions, respectively; η_2 is −1, 1 and 0 for x, y and z directions, respectively; Δ_{L1} is the force parameter for left bearing, whose value is $\cos\alpha_i\sin\theta_i$, $\cos\alpha_i\cos\theta_i$, and 0 for x, y and z directions, respectively; Δ_{R1} is the force parameter for the right bearing, whose value is $\cos\alpha_j\sin\theta_j$, $\cos\alpha_j\cos\theta_j$, and 0 for x , y and z directions, respectively; l_1 and l_2 are

the distances between the bearings and COG of the rotor as shown in Figure 1; Δ_{L2} is the force parameter for left bearing, whose value is $\sin\alpha_i\sin\theta_i$, $\sin\alpha_i\cos\theta_i$, and 0 for x, y and z directions, respectively; Δ_{R2} is the force parameter for the right bearing, whose value is $\sin\alpha_j\sin\theta_j$, $\sin\alpha_j\cos\theta_j$, and 0 for x , y and z directions, respectively; and $\boldsymbol{M}_f$ is the friction torque in the bearings. More details for the matrices and vectors in Eqs. (14) to (17) can be observed in Ref. [29].

3 Results and discussion

The Runge-Kutta method is applied to obtain the results from the proposed model in Section 2. The used calculation parameters are given in Table 1. The axial preload is 20 N. The radial loads along x and y directions are defined as 25, 50, 75 and 100 N, respectively. The time step is 1×10^{-5} s. The initial displacements are 10^{-6} m. The initial velocities are 0 m/s. The bearing damping is typically in the order of $(0.25-2.5)\times10^{-5}$ times the linearized stiffness of the bearing (2.9911×10^7 N/m for the studied ball bearing) [29]. The used damping coefficients are located in this range, whose values for the studied components are 5000 N·s /m.

Table 1 Parameters of studied rotor-ball bearing system

Parameter	Value
Inner race diameter, D_i/mm	49.912
Outer race diameter, D_o/mm	80.088
Pitch diameter, D/mm	65
Ball diameter, D_b/mm	15.081
Inner ring width, B/mm	40
Curvature radius of the outer race, r_o/mm	8.01
Curvature radius of the inner race, r_i/mm	7.665
Number of balls, N_b	8
Internal radial clearance, γ/μm	5
Unload contact angle, α_0/(°)	5.26
Elastic modulus of races and ball materials, E/Pa	2.06×10^{11}
Poisson ratio of races and ball materials, ν	0.33
Rotor mass, M_{ri}/kg	3.5
Mass of housing and outer race, M_{ho}/kg	4.2
Moment of inertia of rotor about x and y axes, I_x and I_y/(kg·m^2)	0.5177
Moment of inertia of rotor about z axis, I_z/(kg·m^2)	0.0044
Position of left bearing from COG, l_1/m	0.0875
Position of right bearing from COG, l_2/m	0.1275
Position of external forces to left bearing, l/m	0.174
Dynamic viscosity, η_{oi}/(Pa·s)	0.37
Viscosity pressure factor, α_{oi}/(m^2·N^{-1})	1.5×10^{-8}
Oil density, ρ_{oi}/(kg·m^{-3})	960

3.1 Effect of frictional force on time- and frequency-domain vibration

Figure 2 gives the effect of the frictional force on the time-domain rotational accelerations of the inner race of the system about x and y directions. Here, the external loads about x, y, and z directions are 50 N. The rotor speed is 3000 r/min. In Figure 2, the time-domain rotational accelerations are greatly affected by the friction force; they are also very different for different friction force calculation methods; moreover, the acceleration waveforms from the calculation methods are similar; however, their amplitudes are very different; the acceleration amplitudes of the system without the friction force are larger than those of the system with the friction force for the studied case; the acceleration amplitudes of the proposed method are larger than those from the Palmgren's and SKF's methods; and the acceleration amplitudes of the Palmgren's method are larger than those of the SKF's method. Some phase differences for the studied calculation methods are also observed. Figure 3 plots the effect of the frictional force on the spectra of the rotational accelerations of the inner race of the system along x and y directions in Figure 2. In Figure 3, a peak frequency occurs at 153.3 Hz in the spectra along the two directions, which is very similar to the ball passing frequency of the outer race (ball passing out raceway frequency BPFO=154.06 Hz, whose calculation method is given in Ref. [39]). Here, the spectra are obtained by using the fast Fourier transform (FFT) method. The same phenomenon is given in Refs. [23, 29], which can give some model validation. Moreover, the amplitude relationships between different friction force calculation methods are similar as those in Figure 2. Note that the friction force in the bearing can affect the spectrum amplitude; however, it cannot affect the bearing characteristic frequency. The differences between the proposed method and Palmgren's method are less than those between the proposed method and SKF's method. It shows that the friction force should be considered during the vibration analysis of the RBHs.

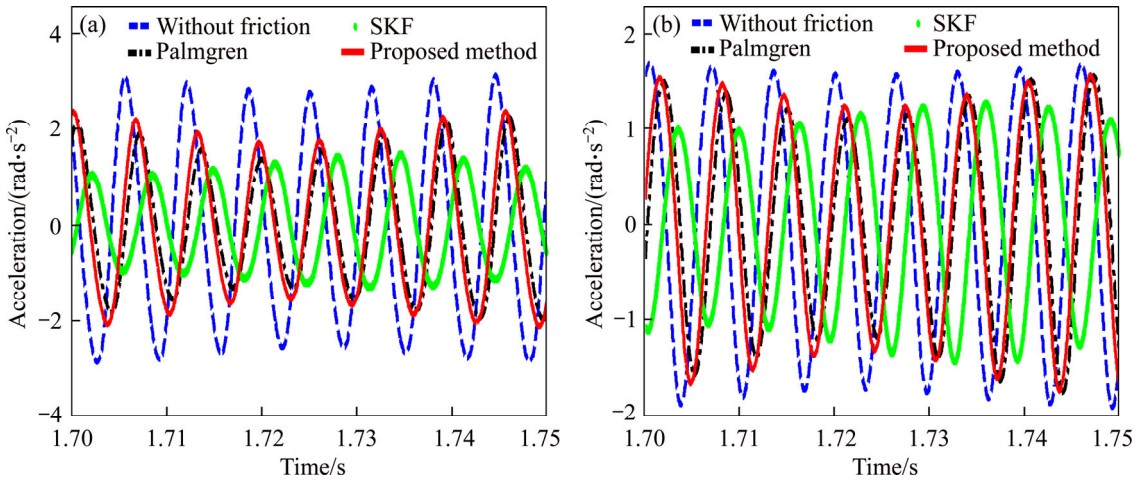

Figure 2 Effect of frictional force on rotational accelerations in x direction (a) and y direction (b)

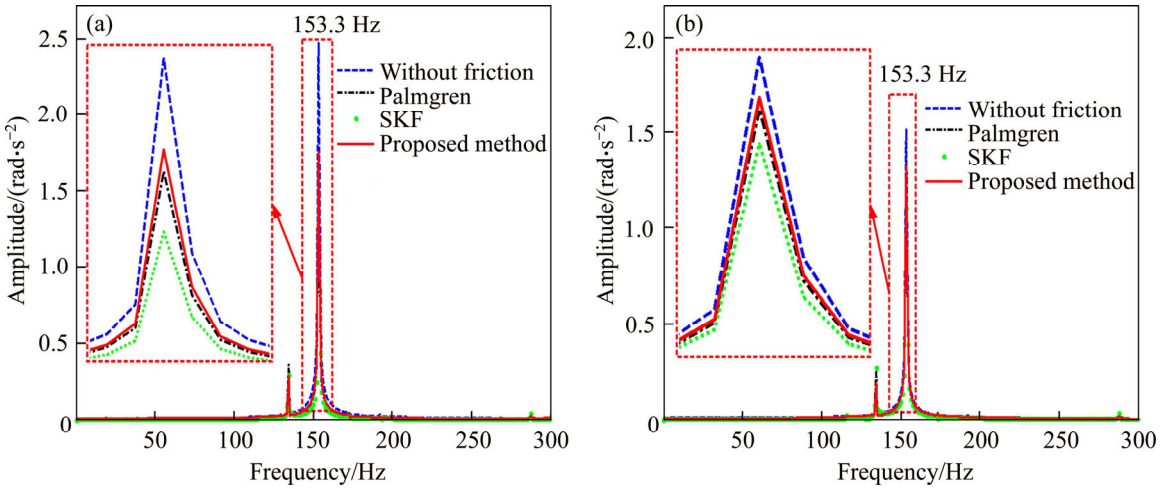

Figure 3 Effect of frictional force on spectra of rotational accelerations in x direction (a) and y direction (b)

3.2 Effects of rotor speed and frictional force on statistics

Figure 4 shows the effects of rotor speed and frictional forces on the statistics including root mean square (RMS) and peak to peak (PTP) values of the rotational accelerations in x direction and y direction. Here, the external loads along x, y and z directions are 50 N. The rotor speed is 1000, 2000, 3000 and 4000 r/min, respectively. In Figure 4, the RMS and PTP values are greatly affected by the rotor speed and friction force. The RMS and PTP values of the rotational accelerations for the models with and without the friction force increase with the rotor speed. When the rotor speed is lower than 2000 r/min, the acceleration amplitudes of the models with the friction force are less than those of the model without the friction force. However, when the rotor speed is higher than 2000 r/min, the acceleration amplitudes of the models with the friction force is more than those of the model without the friction force. When the rotor speed is 1000 r/min, the acceleration amplitudes of the studied models are as follows: Palmgren's method, SKF's method, proposed method, and the model without the friction force. When the rotor speed is 2000 r/min, the acceleration amplitudes of the studied models are as follows: SKF's method, proposed method, Palmgren's method, and the model without friction force. When the rotor speed is larger than 3000 r/min, the acceleration amplitudes of the studied models are as follows: the model without friction force proposed method, Palmgren's method, and SKF's method. Moreover, the differences between the studied friction force calculation methods increases with the rotor speed. Similarly, the results show that the differences between the proposed method and Palmgren's method are less than those between the proposed method and SKF's method. It also seems that the friction force should be considered during the

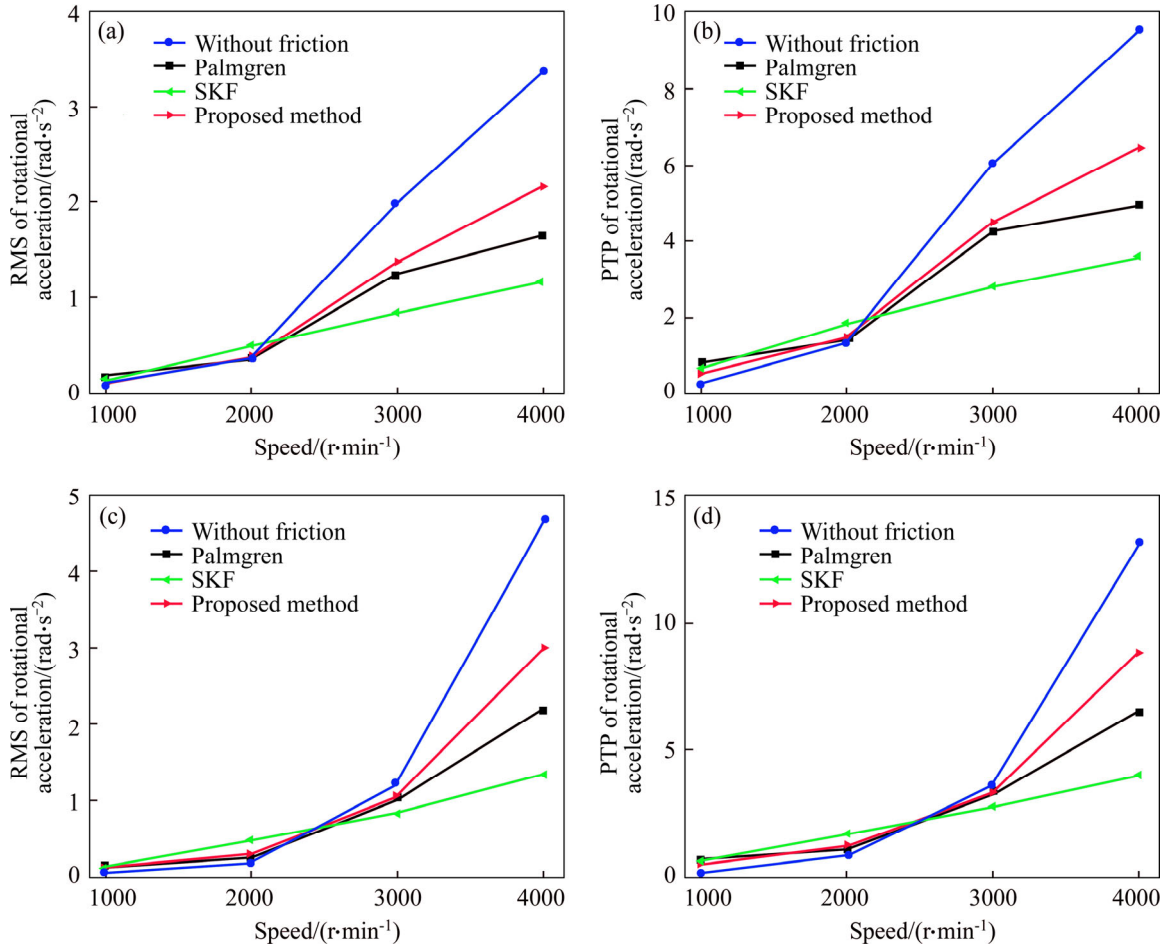

Figure 4 Effects of rotor speed and frictional forces on statistics of rotational accelerations: (a) RMS values for x direction; (b) PTP values for x direction; (c) RMS values for y direction; (d) PTP values for y direction

vibration analysis of the RBHs.

3.3 Effects of external load and frictional force on statistics

Figure 5 depicts the effects of the load and frictional forces on the statistics including RMS and PTP values of the rotational accelerations in x direction and y direction. Here, the rotor speed is 2000 r/min. The external load along x direction is 25, 50, 75 and 100 N, respectively. The external loads along y and z directions are 50 N. In Figure 5, the RMS and PTP values are greatly affected by the external load and friction force. The RMS and PTP values of the rotational accelerations for the models with and without the friction force increase with the external load. The acceleration amplitudes of the models with the friction force is more than those of the model without the friction force. When the external load is from 25 to 50 N, the acceleration amplitudes of the studied models are as follows: SKF's method, proposed method, Palmgren's method, and the model without the friction force. When the external load is from 75 to 100 N, the acceleration amplitudes of the studied models are as follows: proposed method, SKF's method, Palmgren's method, and the model without the friction force. Moreover, the differences between the studied friction force calculation methods increase with the external load. When the external load is from 25 to 50 N, the results show that the differences between the proposed method and Palmgren's method are less than those between the proposed method and SKF's method. When the external load is from 75 to 100 N, the results show that the differences between the proposed method and Palmgren's method are more than those between the proposed method and SKF's method. It also seems that the friction force should be considered during the vibration analysis of the RBHs.

In Figures 2−5, some differences between different friction models are observed. The relative

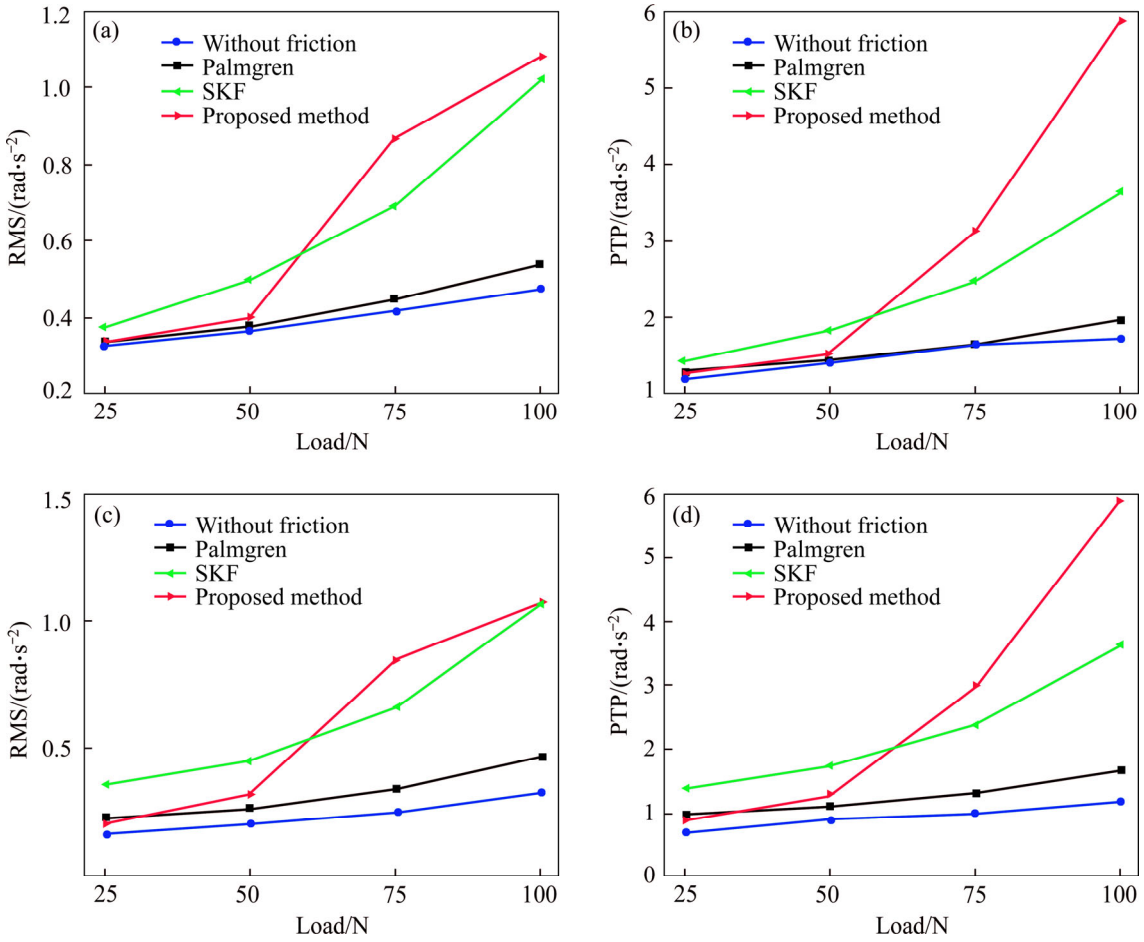

Figure 5 Effects of external load and frictional forces on statistics of rotational accelerations: (a) RMS values for x direction; (b) PTP values for x direction; (c) RMS values for y direction; (d) PTP values for y direction

mechanisms of the differences are discussed as follows. In Palmgren's model, the load dependent and independent factors are considered. However, it only suggests a factor f_1 to formulate the effects of the bearing forces and geometries, which cannot accurately formulate difference force and geometries conditions. It is a whole calculation method, which cannot formulate the details of the friction forces between the mating parts of the bearing system. In SKF model, the rolling, slipping, seal and viscous friction forces are empirically considered; similarly, it only suggests some fixed values for the rolling friction factor, slipping friction factor, and seal friction factor to formulate the effects of the bearing forces and geometries. It cannot completely formulate the details of the friction forces between the mating parts of the bearing system either. In analytical model, the rolling friction moments caused by the elastic material hysteresis, slipping friction moments produced by the differential ones, slipping moment generated by the sliding friction between the cage and ring, and viscous friction moments engendered by the lubricating oil are formulated. It can give a more accurate method to formulate the details of the load dependent and independent friction forces in the bearing system.

4 Conclusions

This study develops an improved dynamic model of a RBS considering different frictional force models. A comparative investigation on the influences of the empirical and analytical frictional force models on the vibration characteristics of the RBS is proposed. The influences of the external load and rotational speed on the vibrations of the RBS are analyzed. The comparative results show that the analytical frictional force model can give a more reasonable method for formulating the effects of the friction forces in the bearings on the vibrations of the RBS. The results also demonstrate

that the friction forces in the bearings can significantly affect the vibrations of the RBSs. The acceleration waveforms from the models with and without the friction force are similar; however, their amplitudes are very different. The friction force in the bearing can affect the spectrum amplitude but the bearing characteristic frequency. The RMS and PTP values of the rotational accelerations for the models with and without the friction force increase with the rotor speed and external load. For a smaller external load, the differences between the proposed method and Palmgren's method are less than those between the proposed method and SKF's method. For a larger external load, the differences between the proposed method and Palmgren's method are more than those between the proposed method and SKF's method. It seems that the friction force should be considered during the dynamic modelling and vibration analysis of the RBHs.

References

[1] LIU J, SHAO Y. Overview of dynamic modelling and analysis of rolling element bearings with localized and distributed faults [J]. Nonlinear Dynamics, 2018, 93(4): 1765−1798. DOI: 10.1007/s11071-018-4314-y.

[2] LIU J, TANG C, WU H, XU Z, WANG L. An analytical calculation method of the load distribution and stiffness of an angular contact ball bearing [J]. Mechanism and Machine Theory, 2019, 142: 103597. DOI: 10.1016/j.mechmachtheory.2019.103597.

[3] PALMGREN A. Ball and roller bearing engineering [M]. 3rd ed. Burbank, Philadelphia: SKF Industries, 1959.

[4] DENG S R, LI X L, WANG J G, TENG H F. Frictional torque characteristic of angular contact ball bearings [J]. Journal of Mechanical Engineering, 2011, 47(5): 114−120.

[5] KAKUTA K. Generating mechanism of friction torque in a ball bearing 2 [J]. Mechanism, 1965, 3: 645−648.

[6] SNARE B. Rolling resistance in lightly loaded bearings [J]. The Ball Bearing Journal, 1968, 152: 3−8.

[7] SNARE B. Rolling resistance in lightly loaded bearings [J]. The Ball Bearing Journal, 1968, 153: 19−24.

[8] SNARE B. Rolling resistance in lightly loaded bearings [J]. The Ball Bearing Journal, 1968, 154: 3−14.

[9] TODD M J, STEVENS K T. Frictional torque of angular contact ball bearings with different conformities [R]. Risley, Technical Report ESA-CR(P)-1221, 1978.

[10] GENTLE R, PASDARI M. Measurement of cage and pocket friction in a ball bearing for use in a simulation program [J]. ASLE Transactions, 1985, 28(4): 536−541. DOI: 10.1080/05698198508981652.

[11] TRIPPETT R. Ball and needle bearing friction correlations under radial load conditions [J]. SAE Tech, 1985, Paper No. 851512. DOI: 10.4271/851512.

[12] CHIU Y, MYERS M. A rotational approach for determining permissible speed for needle roller bearings [J]. SAE Tech, 1998, Paper No. 982030. DOI: 10.4271/ 982030.

[13] SKF. General catalog 4000 [R]. Gothenburg, Sweden: Svenska Kullargerfabriken, 2004.

[14] IQBAL S, BENDER F A, CROES J, PLUYMERS B, DESMET W. Frictional power loss in solid-grease-lubricated needle roller bearing [J]. Lubrication Science, 2013, 25(5): 351−367. DOI: 10.1002/ls.1195.

[15] LIU J, YAN Z, SHAO Y. An investigation for the friction torque of a needle roller bearing with the roundness error [J]. Mechanism and Machine Theory, 2018, 121: 259−272. DOI: 10.1016/j.mechmachtheory.2017.10.028.

[16] LIU J, LI X, DING S, PANG R. A time-varying friction moment calculation method of an angular contact ball bearing with the waviness error [J]. Mechanism and Machine Theory, 2020, 148: 103799. DOI: 10.1016/j.mechmachtheory.2020.103799.

[17] TONG V C, HONG S W. Study on the running torque of angular contact ball bearings subjected to angular misalignment [J]. Journal of Engineering Tribology, 2018, 232(7): 890−909. DOI: 10.1177/1350650117732921.

[18] HAN Q, DING Z, QIN Z, WANG T, XU X, CHU F. A triboelectric rolling ball bearing with self-powering and self-sensing capabilities [J]. Nano Energy, 2020, 67: 104277. DOI: 10.1016/j.nanoen.2019.104277.

[19] HAN Q, DING Z, XU X, WANG T, CHU F. Stator current model for detecting rolling bearing faults in induction motors using magnetic equivalent circuits [J]. Mechanical Systems and Signal Processing, 2019, 131: 554575. DOI: 10.1016/j.ymssp.2019.06.010.

[20] XU T, YANG L, WU Y. Friction torque study on double-row tapered roller bearing [C]// 2019 IEEE International Instrumentation and Measurement Technology Conference (I2MTC). Auckland, New Zealand: IEEE, 2019: 18974243.

[21] KWAK W, LEE J, LEE Y B. Theoretical and experimental approach to ball bearing frictional characteristics compared with cryogenic friction model and dry friction model [J]. Mechanical Systems and Signal Processing, 2019, 124: 424−438. DOI: 10.1016/j.ymssp.2019.01.056.

[22] BABU C K, TANDON N, PANDEY R K. Vibration modeling of a rigid rotor supported on the lubricated angular contact ball bearings considering six degrees of freedom and waviness on balls and races [J]. Journal of Vibration and Acoustics, 2012, 134(1): 011006. DOI: 10.1115/1.4005140.

[23] BABU C K, TANDON N, PANDEY R K. Nonlinear vibration analysis of an elastic rotor supported on angular contact ball bearings considering 6 DOF and waviness on balls and races [J]. ASME Journal of Vibration and Acoustics, 2014, 136: 044503. DOI: 10.1115/1.4027712.

[24] LIU J, SHAO Y M, MING J Z. The effects of the shape of localized defect in ball bearings on the vibration waveform [J]. Journal of Multi-body Dynamics, 2013, 227(3): 261−274. DOI: 10.1177/1464419313486102.

[25] LIU J, SHAO Y M, ZHU W D. A new model for the relationship between vibration characteristics caused by the time-varying contact stiffness of a deep groove ball bearing and defect sizes [J]. ASME Journal of Tribology, 2015, 137(3): 031101. DOI: 1.4029461.

[26] CAO H, NIU L, XI S, CHEN X. Mechanical model

development of rolling bearing-rotor systems: A review [J]. Mechanical Systems and Signal Processing, 2018, 102: 37−58. DOI: 10.1016/j.ymssp.2017.09.023.

[27] CAO H, LI Y, CHEN X. A new dynamic model of ball-bearing rotor systems based on rigid body element [J]. Journal of Manufacturing Science and Engineering, 2016, 138(7): 071007. DOI: 10.1115/1.4032582.

[28] HALMINEN O, ACEITUNO J F, ESCALONA J L, SOPANEN J, MIKKOLA A. A touchdown bearing with surface waviness: Friction loss analysis [J]. Mechanism and Machine Theory, 2017, 110: 73−84. DOI: 10.1016/j.mechmachtheory.2017.01.002

[29] LIU J, SHAO Y. Dynamic modeling for rigid rotor bearing systems with a localized defect considering additional deformations at the sharp edges [J]. Journal of Sound and Vibration, 2017, 398: 84−102. DOI: 10.1016/j.jsv.2017.03.007.

[30] LIU J. A dynamic modelling method of a rotor-roller bearing-housing system with a localized fault including the additional excitation zone [J]. Journal of Sound and Vibration, 2020, 469: 115144. DOI: 10.1016/j.jsv.2019.115144.

[31] NEISI N, HEIKKINEN J E, SOPANEN J. Influence of surface waviness in the heat generation and thermal expansion of the touchdown bearing [J]. European Journal of Mechanics-A/Solids, 2019, 74: 34−47. DOI: 10.1016/j.euromechsol.2018.10.014.

[32] XU L X, CHEN B K, LI C Y. Dynamic modelling and contact analysis of bearing-cycloid-pinwheel transmission mechanisms used in joint rotate vector reducers [J]. Mechanism and Machine Theory, 2019, 137: 432−458. DOI: 10.1016/j.mechmachtheory.2019.03.035.

[33] ZHENG D, CHEN W, XIAO G, ZHENG D. Effect of vibration on power loss of angular contact ball bearings [J]. Industrial Lubrication and Tribology, 2019, DOI: 10.1108/ILT-06-2019-0217.

[34] POPESCU A, HOUPERT L, OLARU D N. Four approaches for calcuting power losses in an angular contact ball bearing [J]. Mechanism and Machine Theory, 2020, 144: 103669. DOI: 10.1016/j.mechmachtheory.2019.103669.

[35] HAMMAMI M, MARTINS R, FERNANDES C, SEABRA J, ABBES M S, HADDAR M. Friction torque in rolling bearings lubricated with axle gear oils [J]. Tribology International, 2018, 119: 419−435. DOI: 10.1016/j.triboint.2017.11.018.

[36] ZHANG X, XU H, CHANG W, XI H, XING Y, PEI S Y, WANG F C. Torque variations of ball bearings based on dynamic model with geometrical imperfections and operating conditions [J]. Tribology International, 2019, 133: 193−205. DOI: 10.1016/j.triboint.2019.01.002.

[37] MAJDOUB F, SAUNIER L, SIDOROFF-COICAUD C, MEVEL B. Experimental and numerical roller skew in tapered roller bearings [J]. Tribology International, 2020, 145: 106142. DOI: 10.1016/j.triboint.2019.106142.

[38] HARRIS T A, KOTZALAS M N. Rolling bearing analysis-essential concepts of bearing technology [M]. 5th ed. New York: Taylor and Francis, 2007.

[39] LYNAGH N, RAHNEJAT H, EBRAHIMI M, AINI R. A bearing induced vibration in precision high speed routing spindles [J]. International Journal of Machine Tools and Manufacture, 2000, 40: 561−577. DOI: 10.1016/S0890-6955(02)00049-4.

(Edited by FANG Jing-hua)

中文导读

考虑不同摩擦力模型的转子–轴承系统振动特性研究

摘要：轴承各部件之间的摩擦力直接影响转子–轴承系统的振动特性。因此，深入研究轴承摩擦力对转子系统振动的影响将有助于解释转子系统的振动机理。本文提出了一种考虑不同摩擦力模型的改进转子–轴承系统动力学模型。研究了经验摩擦力模型和解析摩擦力模型对转子–轴承系统振动特性的影响规律。经验摩擦力模型包括 Palmgren 模型和 SKF 模型。分析摩擦力模型考虑了径向弹性材料迟滞引起的滚动摩擦、球与滚道之间的滑动摩擦、润滑油引起的粘性摩擦、球与保持架之间的接触摩擦。分析了外载荷和转速对系统振动特性的影响规律。结果表明，本文所建立的分析摩擦力模型可以为研究轴承摩擦力对转子–轴承系统振动特性的影响规律提供一种更合理的方法；轴承内的摩擦力对转子–轴承系统的振动特性有显著的影响。

关键词：摩擦力；振动特性；转子–轴承系统；动力学模型